First publ. in: Physica Scripta, T22 (1988), pp. 98-101

A Scheme for Measuring the Neutrino Rest Mass from the β-Decay of Stored Tritium Atoms Using a Solenoid Retardation Spectrometer

H. Backe, J. Bonn, Th. Edling, H. Fischer, A. Hermanni, P. Leiderer, Th. Loeken, R. B. Moore,* A. Osipowicz, E. W. Otten and A. Picard

Institut für Physik, Johannes Gutenberg-Universität Mainz, D-6500 Mainz, Fed. Rep. of Germany, and *Foster Radiation Laboratory, McGill University Montreal, Canada

Received October 29, 1987; accepted January 15, 1988

Abstract

A new type of electron spectrometer is under construction at Mainz University that allows a measurement of the β-spectrum of tritium with high resolution and transmission in order to determine the neutrino rest mass. It consists of a source that contains atomic tritium, trapped in a high magnetic field, and a solenoid retarding spectrometer

1. Introduction

The question of a finite neutrino mass has penetrated in recent years almost any field of physics. It concerns the fundamental concepts of elementary particle physics as well as those of astrophysics. Much more spread, even, is the experimental interest in measuring the neutrino mass. The great number of different attempts may be grouped into two classes: (1) direct mass measurement from weak decay spectra; (2) indirect measurement from (a) ν-oscillations and (b) neutrino-less double β-decay. Our experiment, belonging to the first group, addresses itself in particular to the classical problem of determining the $\bar{\nu}_e$-mass from the β-decay spectrum of tritium near its endpoint at 18.6 keV. There, it is conveniently expressed in terms of the dimension-less quantity,

$$\varepsilon = (Q_0 - E)/m_\nu, \tag{1}$$

i.e., the difference between the total decay energy Q_0 and the electron energy E in units of an assumed $\bar{\nu}_e$-mass m_ν. The differential decay rate near the endpoint is then approximately given by

$$dR(\varepsilon) = S(\varepsilon)\, d\varepsilon \sim 1 \times 10^{-11}\, R(m_\nu/\mathrm{eV})^3 \times (\varepsilon\sqrt{\varepsilon^2 - 1})\, d\varepsilon, \quad \varepsilon > 1, \tag{2}$$

where R is the total decay rate and m_ν is taken in electron volts. The function in brackets approaches the limit $\varepsilon^3 - \frac{1}{2}$ for $\varepsilon \gg 1$. It is to be replaced by ε^2 for all $\varepsilon > 0$ if the neutrino mass is in fact zero. The significance of a possible $\bar{\nu}_e$-mass in $dR(\varepsilon)$ is practically limited to the range $\varepsilon \lesssim 3$ which contains a fractional decay rate of only

$$\Delta R(\varepsilon \leqslant 3)/R \sim 10^{-13}(m_\nu/\mathrm{eV})^3. \tag{3}$$

For larger ε the $\bar{\nu}_e$-mass causes a small, but constant offset of the spectrum which is getting lost in the fluctuations of the rapidly increasing count rate.

Besides the obvious count rate problem the experiment faces two more basic difficulties: (1) The deterioration of the endpoint spectrum by final state interaction in a solid target; (2) the resolution of the β-spectrometer which preferably should resolve the significant part of the spectrum (2) as well as the final state effects. In experiments, using traditional magnetic spectrometers, the two latter problems are coupled to the count rate problem by the unfortunate circumstance that a higher resolution of the instruments can be gained only on cost of their transmission. The difficulty of analyzing endpoint spectra which have a debatable structure with respect to the final state effects and which have been measured with limited statistics and resolution only, has led to the present controversy in the literature, where one group insists on a finite mass [1]

$$17\,\mathrm{eV} \leqslant m_{\bar{\nu}_e} \leqslant 40\,\mathrm{eV}$$

whereas its strongest opponent quotes a null result [2]

$$m_{\bar{\nu}_e} \leqslant 18\,\mathrm{eV} \quad (95\%\ \mathrm{c.l.}).$$

A recent attempt to avoid the problem of spectral deterioration in a solid by use of a gaseous tritium target yielded a value of [3]

$$m_{\bar{\nu}_e} \leqslant 26.8\,\mathrm{eV} \quad (95\%\ \mathrm{c.l.}).$$

It corroborates the result of Ref. [2] but still faces the problem of statistics in view of the small transmission of the spectrometer and the rather limited source strength.

The experimental scheme described in this paper tries to attack the three basic problems of spectral deterioration, low transmission and limited resolution by a completely different approach. First ideas in this direction were stimulated by the successful experiments to store samples of about 10^{16} spin-polarized ^{1}H-atoms in a magnetic trap at low temperature [4, 5] which might solve the source problem when applied to ^{3}H. Thinking the case over, it turned out that the trapping magnet might also form the basic element of an almost ideal spectrometer as described below. While preparing this experiment the same idea has been published by Lobashev *et al.* [6].

2. Principle of a source of trapped spin-polarized ^{3}H-atoms

The atomic hydrogen trap mentioned in the introduction follows a hybrid trapping scheme (compare Fig. 1, left side). Axial confinement is achieved by the Stern–Gerlach potential of an inhomogeneous magnetic field of 8–10 Tesla central strength. It stores hydrogen atoms with negative electron spin projection at thermal energies not exceeding ~1 Kelvin. Those with positive spin projection are expelled from the trap. Radial confinement is provided by a cylinder covered

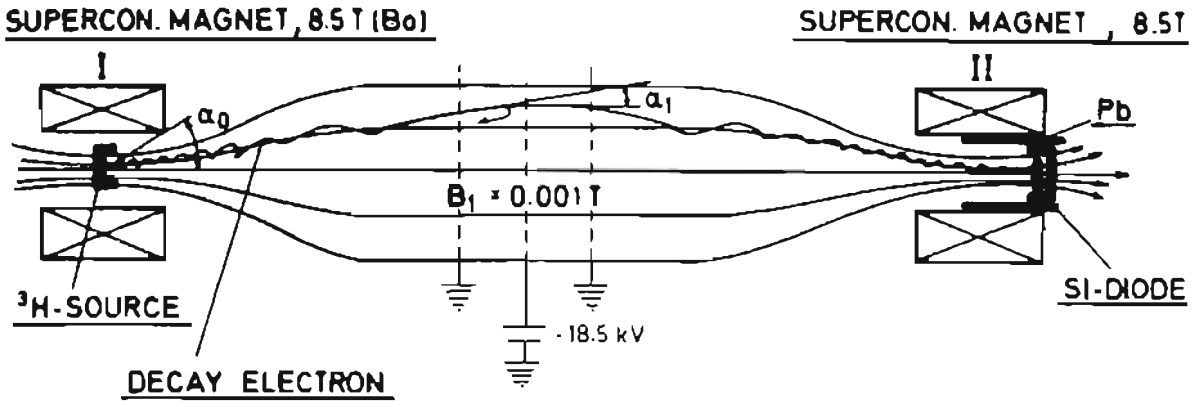

Fig. 1. Principle of a solenoid retardation spectrometer for analyzing the endpoint spectrum of the β-decay from a magnetically trapped atomic tritium source. Left: T-container covered with suprafluid He and placed in the centre of an inhomogeneous 8 T field. Middle. Electrostatic filter placed in a weak magnetic field of about 10^{-3} T. Right. Second 8 T field reconcentrating the flux of transmitted β-particles onto the detector.

with a superfluid He film on which atomic hydrogen will not condense at any temperature. Thus the atoms could only be lost by recombination. This does not occur in a spin-polarized gas, however, since the triplet states of the H_2-molecule are unbound. This way, it was possible to store hydrogen atoms at densities of $10^{16}/cm^3$ for times of hours [7, 8]. Applied to tritium this scheme would obviously provide an ideal source for measuring the endpoint spectrum. However, physical chemistry of tritium at low temperatures is distinctly different from that of hydrogen due to the reduced zero point motion of the former. Calculations indicate that atomic tritium is probably still unbound by a few K in bulk liquid He with respect to the vacuum state. But the calculations also show the existence of bound surface states for tritium into which most of atoms may condensate at low temperature in constrast to the hydrogen case. The question has to be settled by experiments which are underway elsewhere [9]. To begin with we consider, therefore, a frozen T_2-source for which final state effects seem to be calculable with sufficient precision [10].

3. Principle of a solenoid retardation spectrometer

With the source placed in the centre of a solenoid, a decay electron will spiral into the low field region along and around the particular field line at which it was born (compare Fig. 1). On its path into low field, the electron will be accelerated axially on cost of the transverse energy of its cyclotron motion. In case of adiabatic motion (i.e., the relative change of the magnetic field during one cyclotron period is everywhere much smaller than 1), the transverse kinetic energy is reduced by the same factor by which the field has dropped:

$$E_1^{\perp}/E_0^{\perp} = B_1/B_0. \qquad (4)$$

Let us assume the ratio $B_1/B_0 = 10^{-3}\,\mathrm{T}/9\,\mathrm{T}$, then the maximum possible value of $E_1^{\perp}$ would be 2 eV for an electron starting with a total energy of 18 keV at B_0. Assuming B_1 being a homogeneous field, furthermore, one could retard the electrons in an electric field of a double condenser, formed by 3 parallel grids, e.g., Setting the central grid at the potential $-U$, all electrons with a parallel kinetic energy $E_1^{\parallel} > eU$ would pass the grid. They would then be re-accelerated in the second half of the condenser and be refocussed on a detector by a second solenoid (see Fig. 1). Since E_1 differs from the total starting energy $E_1^{\parallel} + E_0^{\perp}$ by no more than 2 eV for any direction of decay into the forward hemisphere, the transmission of the electrostatic filter would drop from 1 to 0 within that energy interval.

It thus combines the advantages of very high resolution and optimum transmission. Its integral way of functioning would not be disturbing, really, since one would operate it anyhow close to the endpoint only where the uninteresting low energy part of the spectrum is rejected.

However, a design as sketched in Fig. 1 contains some serious dangers and drawbacks:

(1) The grids and, in particular, the central electrode represent an uncalculable and probably fatal source of background. Because electrons emerging from these grids by the decay of any adsorbed tritium contamination or by secondary emission due to cosmics will reach the detector unfiltered. Therefore, the magnetic flux tube within which the electrons are transported from the source to the detector should not contain any matter and should be kept at ultrahigh vacuum. On the other hand, this solenoidal transport system protects the detector from any background electrons originating from somewhere outside the flux tube (e.g., from the walls of the vacuum tank), since these electrons will spiral along a field line by-passing the detector area. This is an advantage over conventional, purely electrostatic filters.

(2) If the electrons were guided at full energy into the low field region, their spiral motion would stretch out to an almost straight line. Consequently the adiabaticity criterium could be fulfilled only at very small magnetic field gradients, requiring an enormous length of the apparatus.

It is preferable, therefore, to decelarate electrostatically the logitudinal motion already in the transition region from high to low B-field such that the longitudinal acceleration by the magnetic field gradient is just compensated. In order not

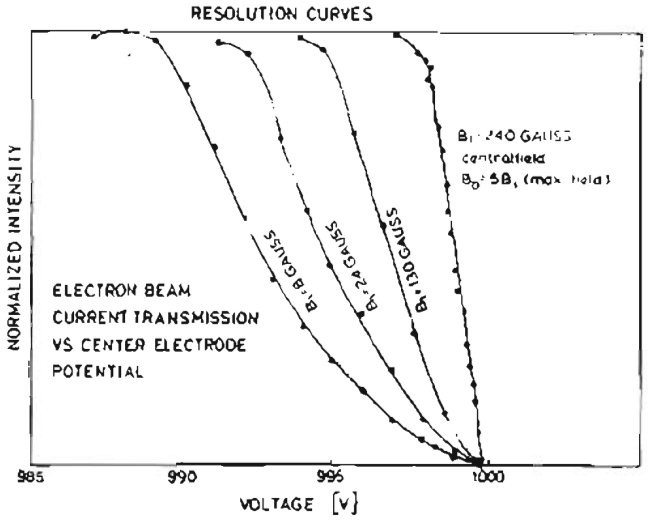

Fig. 2. Transmission function of an 1 keV test spectrometer, measured as a function of the central guiding field B_1 [11]

to deflect the electrons, the E-lines should in principle be always parallel to the B-lines. But this condition is relaxed considerably by the stabilizing action of the (much stronger) Lorentz force which limits the side drift of the electron to stay within the diameter of the well-known rosette of magnetron motion. This effect has been demonstrated recently in a pilot experiment, where a 1 keV electron beam passed an electrostatic filter. It consisted of a series of ring electrodes with the maximum potential on the central one. Parallel to the beam axis an inhomogeneous magnetic field was applied which decreased by a factor five on the way from the electron source to the central electrode in order to parallize the electron beam. Figure 2 shows the filter transmission as a function of the central potential for different values of the magnetic field strength (measured at its minimum value in the centre). One observes that the half width decreases from about 5 to 1 eV by increasing the field from 8 to 240 G [11]. The electron behaves just like a bullet – so to say – the path of which is the stiffer the faster it spins. It can be shown, moreover, that in a magnetic monopole field the electron motion is strictly adiabatic in the sense of eq. (4), irrespective of the large gradient ($\sim 1/r^2$) of such a field [12]. A magnetic monopole field is realized approximately around the front end of a solenoid. The corresponding electric monopole field for longitudinal deceleration can be generated by a series of ring electrodes whose diameter and potential increase outwards.

Figure 3 shows the arrangement of electrodes. In the upper part are the front electrodes, facing the solenoid, in the lower one the central electrodes where the repelling potential attains its maximum value. Shown is only a cross section through the upper left sector of the spectrometeer which observes cylindrical symmetry around the z-axis and mirror symmetry with respect to its central plane at $z = 195$ cm. The dashed line gives the magnetic field strength on the z-axis as produced by the two solenoids placed at both ends of the spectrometer. One contains the source, the other the detector

The decisive equipotential lines near the center of the spectrometer are plotted with a spacing of 1 V in the lower right part of Fig. 3. They prove that the variation of the maximum potential (18 000 V) in the symmetry plane (i.e., the central potential hole) is of the order of 1 eV only thus enabling a very high resolution over the full plane of the spectrometer. This high constancy of the central potential is achieved by virtue of this special design which keeps the front electrodes (being dangerous because of its very different potential) small and well-shielded by the intermediate ones.

We conclude this section by presenting some results of numerical calculations of particle trajectories performed with the well-known Herrmannsfeldt program [13]. It was modified, however, in order to facilitate the Runge–Kutta integration of the trajectory which has an extremely strong curvature in a fixed coordinate system due to the large Lorentz force. This requires a very large number of integration steps. It was advisable, therefore, to integrate the equation of motion in an accompanying cylindrical coordinate frame which is aligned everywhere to th particular magnetic field line around which the electron spirals. In this system the asimuth $[\varphi(z)]$ and the radius $[r(z)]$ of the trajectory vary only smoothly with the propagation along the actual z-axis [14].

Figure 4 shows the check of the adiabatic transformation of transverse energy according eq. (4) along a typical trajec-

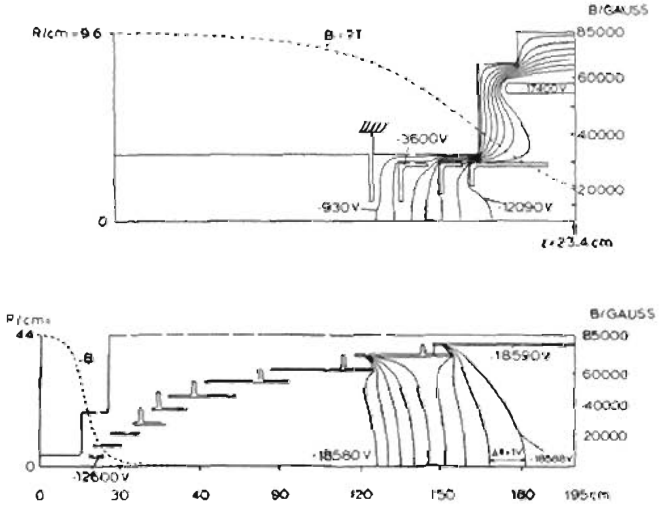

Fig. 3. Configuration of electrodes and fields of the solenoid retardation spectrometer under construction. Further explanations in the text. Dimensions are given on the r- and z-axis; on the right ordinate also the scale of the B-field on the z-axis (dashed curve)

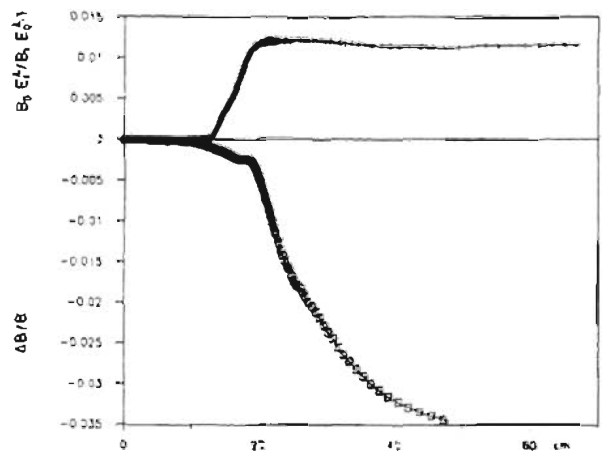

Fig. 4. Numerical check of adiabacity. Lower curve: Relative change of magnetic field $\Delta B/B$ per cyclotron period. Upper curve: Violation of adiabacity as measured by the function $B_0/B_1 \cdot E_\perp/E_\perp - 1$. Beyond $z = 60$ cm it levels off. With respect to $E_1^\perp$ it corresponds to a deviation of $\Delta E^\perp \sim 0.1$ V at the right end of the diagram

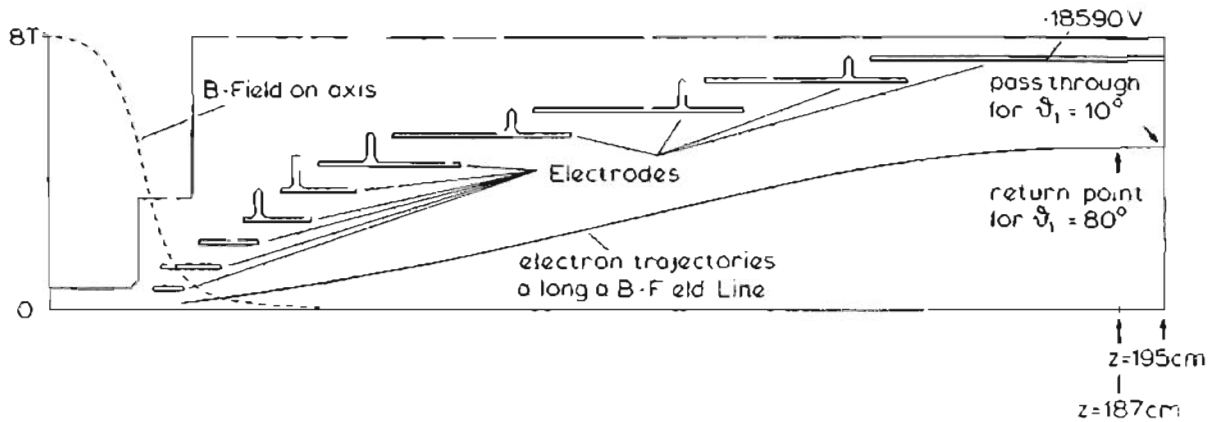

Fig. 5. Two critical electron trajectories, both starting off axis with a total energy E_0 being ~ 1 eV above the central potential barrier at $z = 197$ cm. The one starting with polar angle $\vartheta = 10°$ passes the barrier, the one starting with $\vartheta = 80°$ is reflected at $z = 187$ cm, a fraction of a Volt below the maximum of the barrier.

tory through the field configuration of Fig. 3. One remarks that the violation of eq. (4) never exceeds a few percent which is quite satisfactory. Thus the calculation insures that the spectrometer will indeed reach the proposed steep transmission function which drops from 1 to 0 within an energy range of

$$\Delta E \sim E_1^{\perp} \sim E_0 B_1/B_0 \qquad (5)$$

which is about $10^{-4} E_0$ for the field configuration considered. This is further demonstrated by the two calculated trajectories shown in Fig. 5. In both cases the electron starts with the same total energy E_0 chosen about 1 eV above the filter potential. The one, emitted with a polar angle $\vartheta = 80°$, is reflected just before the symmetry plane at a potential of about 0.5 V below the maximum one, whereas the one starting with $\vartheta = 10°$ passes the filter.

4. Status of the experiment

The design of the spectrometer has been finished early in 1987. The spectrometer tank and the superconducting solenoids have been delivered this summer. The whole set-up including a solid T_2-target, containing about 10^{16} T_2 atoms, and a suitable detector are expected to be ready for running by the end of this year.

References

1. Boris, S. *et al.*, Phys. Rev. Lett. **58**, 2019 (1987).
2. Kündig, W. *et al.*, Phys. Lett. **B173**, 485 (1986).
3. Wilkerson, J. F. *et al.*, Phys. Rev. Lett. **58**, 2023 (1987).
4. Walraven, J. T. M. *et al.*, Phys Rev. Lett. **45**, 449 (1980).
5. Kleppner, D. *et al.*, Phys. Rev. Lett. **47**, 1195 (1981).
6. Lobashev, V. M. *et al.*, Nucl. Instr. Meth. **A240**, 305 (1985).
7. Greytak, T. J. and Kleppner, D., in New Trends in Atomic Physics, p. 1125 (Edited by S. Grynberg and R. Stora), Les Houches Session XXXVIII 1982 (1984).
8. Silvera, I. F. and Walraven, J. T. M., in Progress in Low Temperature Physics, Vol. X, North Holland, Amsterdam, in print.
9. Hardy, W. N. *et al.*, Private communication.
10. Fackler, O. *et al.*, Phys. Rev. Lett. **55**, 1388 (1985).
11. Moore, R. B., Private communication.
12. Lehnert, B., Dynamics of Charged Particles, Amsterdam (1964).
13. Description of the Program in Electron Trajectory Program, W. B. Herrmannsfeldt, SLAC Report-226, Nov. (1979).
14. Description of the Altered Ray Traceing Routine, in Diplomarbeit, Th. Edling, Institut für Physik der Universität Mainz (1987).